EPJ Web of Conferences **250**, 06012 (2021) https://doi.org/10.1051/epjconf/202125006012
DYMAT 2021

Dynamice fracture in a semicristalline polymer: an analysis of the fracture surface

Jean-Benoît Kopp[1,*] and *Jérémie* Girardot[1]

[1]Arts et Metiers Institute of Technology, Univ. of Bordeaux, CNRS, Bordeaux INP, INRAE, HESAM Université, I2M Bordeaux, F-33400 Talence, France

Abstract. The fracture behaviour of a specific material, a semi-crystalline bio-based polymer, was here studied. Dynamic fracture tests on strip band specimens were carried out. Fracture surfaces were observed at different scales by optical and electron microscopy to describe cracking scenarios. Crack initiation, propagation and arrest zones were described. Three distinct zones are highlighted in the initiation and propagation zone: a zone with conical markings, a mist zone and a hackle zone. The conical mark zone shows a variation in the size and density of the conical marks along the propagation path. This is synonymous with local speed variation. Microcracks at the origin of the conical marks in the initiation zone seem to develop from the nucleus of the spherulites. In the propagation zone with complex roughness, the direction of the microcracks and their cracking planes are highly variable. Their propagation directions are disturbed by the heterogeneities of the material. They branch or bifurcate at the level of the spherulites. In the arrest zone, the microcracks developed upstream continue to propagate in different directions. The surface created is increasingly smoother as the energy release rate decreases. It is shown that the local velocity of the crack varies in contrast to the macroscopic speed.

1 Introduction

There are numerous studies in the literature on the fracture behaviour of materials and structures [1] [2] [3] [4] [5] [6] [7] [8]. When a cracking mechanism is studied in the laboratory, it is generally to describe the different mechanisms observable at different scales, to quantify the fracture parameters that will feed predictive models or to validate a numerical model (or method). From the micro- to the macro-scale, the description of the mechanisms is necessary although complex. This makes it possible to rigorously evaluate and predict the mechanisms that may lead to the collapse of a structure. Indeed, the appearance of micro- and macro-cracks is largely correlated to the microstructure and heterogeneities of the material, the mechanical stress or even the effects of the environment [5]. Due to its criticality, the dynamic fracture mechanism is mainly studied in mode I (opening mode). In dynamic regime and for most materials, the size of the fracture process zone remains negligible compared to the crack length. The formalism of linear elastic fracture mechanics (LEFM) can be generally used. It advises a global approach with the energy release rate G or local with the stress intensity factor K. This can be very different for a supposedly

*e-mail: jean-benoit.kopp@ensam.eu

ductile material when a crack propagates slowly. In this last case, the formalisms of fracture mechanics then suggest a local approach with the contour integral J [9].

The fracture behaviour of polymeric materials has been extensively studied in the literature. Environmental effects (temperature and strain rate for example) can significantly modify the emerging behaviour of the material [10] [11]. By increasing the strain rate, a polymer can change from a visco-elastic plastic ductile to an elastic brittle behaviour. Studying the resistance to initiation (or slow propagation) or to rapid propagation can be significantly different for the same polymer material. The formalisms of fracture mechanics also. Homalite 100 and polymethylmethacrylate (PMMA) have regularly served as model materials for studying materials with brittle linear elastic behaviour. Their fracture facies have been widely described. Different characteristic zones exist. At crack initiation, conical markings can be observed [12] [13] [14]. They result from the interaction between a macro crack front and micro crack fronts that develop downstream of the main crack. The analysis of these marks in terms of density and size makes it possible to estimate the crack velocity [15]. During the rapid propagation of the crack, the fracture surface is known as a hackle zone. This zone is chaotic in terms of roughness. Micro-branches, which Sharon and Fineberg [16] describe as the origin of non-trivial roughness, develop from a critical speed. Between these two zones (initiation and propagation) there is an intermediate zone, called mist. For homalite 100, it is established that in the mist zone, several small cracks propagate simultaneously and the front of the overall crack is almost straight [17]. In the hackle zone, crack growth occurs by the same physical process as in the mist zone, except that the size scale of the microfracturing increases. For PMMA, it has been observed that in the hackle zone, and for cracking speeds above about 500 m/s, the fracture surface becomes very rough with periodic microbranch-induced marks [18]. They generate arrest marks spaced about 1 mm apart, commonly called "ribs markings" because of their geometrical shapes. The high roughness observed in the hackle areas is generally not taken into account in the estimation of the fracture energy. It is nevertheless admitted that the higher the energy release rate, the rougher the fracture surface is [19] [20] [10] [11].

In this work, dynamic fracture tests were performed on strip band specimens (SBS) of a bio-based semicrystalline polymer. The material under investigation is relatively undescribed in the literature in terms of the fracture mechanism and especially in dynamic. More generally, the link between the specific microstructure of semi-crystalline polymers and cracking mechanisms at micro-scale is poorly referenced. The fracture surface were analyzed by optical and electron microscopy in different zones (initiation - propagation - arrest) in order to propose cracking scenarios related to the microstructure of semicrystalline polymer. The link between the mechanisms observed at different scales with the local and global cracking velocity and the fracture energy is discussed.

2 Material and methods

2.1 Material

The material studied is polyamide 11 (PA11), the Rilsan BESNO TL grade supplied by Arkema. The strip band specimens were machined from pre-injected plates. The dynamic modulus E_d was obtained by measuring the average ultrasonic velocity in the material $< v_u >$ which is equal to 2100±46 m s^{-1}. As a dynamic modulus, it can be also taken as the 'relaxed' modulus of the material which avoid viscous effect in the estimation of the internal energy (see equation (2)). The value E_d = 1620±82 MPa is obtained from the equation (1), where

ν=0.43 and ρ=1040 kg m^{-3}. For the estimation of the fracture energy in dynamic propagation regime, only E_d and ν will be considered to describe the behaviour of the material [21].

$$E_d = \rho v_u^2 \frac{(1+\nu)(1-2\nu)}{1-\nu} \tag{1}$$

2.2 Dynamic fracture test

The strip band specimen (SBS) geometry [10, 22, 23] is used to study rapid crack propagation (RCP) and crack arrest in PA11 plates. This geometry allows precise control of the boundary conditions during propagation. It generates very few inertia effects induced by rapid crack propagation. An experimental device based on these studies [10, 19, 20] has been designed.

Two notched head-to-tail plates are prestressed (see Fig. 1). One plate is cracked (the plate **1**). The second one ensures the symmetry of the load during propagation. The specimens are initially uniaxially prestressed to a constant deformation using a universal tensile-compression machine. The loading is imposed by moving the crosshead. Once the prestress is reached, the displacement is maintained. The system is then locked by means of nuts mounted on 4 threaded rods. The rods pass through the jaws. The nuts stop the jaws to block the movement in the axis of the rods. The flexibility of the system is then limited. The stop of the crack is generated on the plate **1**. This plate is deliberately longer than the jaw such that an unloaded zone exists. The energy release rate is almost nil and therefore very significantly lower than the fracture energy of the material. The crack is stopping at this zone and to access this arrest zone, the plate was cut with a band saw.

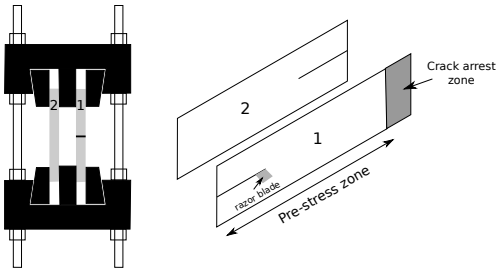

Figure 1. Strip band specimen loading system.

Crack initiation is generated by the impact of a mass on a razor blade in contact with the tip of the crack. The test is carried out at ambient temperature. Six polyamide plates were cracked. The dimension of the plates is: L=300 mm (length), H=80 mm (height), b=4 mm (thickness) and l_n=120 mm (notch length). A single crack propagation perpendicular to the loading axis is shown in Fig. 2. The quasi-static energy release rate in mode I, noted G_{I0}, is defined as a function of the stress σ_{zz} (z is the direction of transverse crack propagation) by considering a plane stress state and the propagation of a single longitudinal crack (see Eq. 2).

$$G_{I0} = \frac{H\sigma_{zz}^2(1-\nu^2)}{2E} \tag{2}$$

A dynamic correction must be considered to estimate the energy release rate in dynamic regime, noted G_{ID}. The average crack velocity is required. A fast camera or a conductive coating [19, 24] can be used to access the spatio-temporal data of the crack tip during propagation. The average velocity of the crack tip for this polymer is approximately 400 ms^{-1}

$\approx 0.6c_R$. The Rayleigh wave velocity (c_R) in PA11 is about 698 ms^{-1} [11]. It is known that the dynamic correction classically used for fast propagation which gives the factor $k = 1 - \frac{\dot{a}}{c_R}$, is unsatisfactory in the case of a *SBS* [3] test. A numerical model adapted to this specimen geometry has been implemented in [19] which gives a small dynamic correction of 10 % which must be considered at $0.6c_R$.

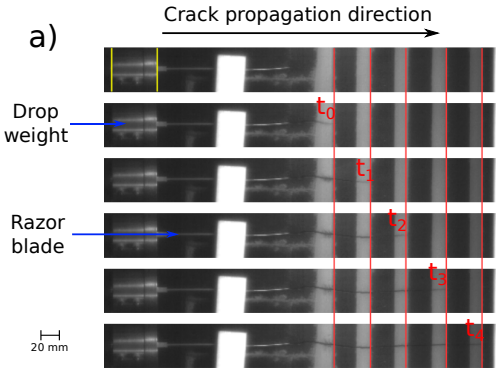

Figure 2. Fast camera images obtained with a sampling rate of 10^4 frames per second to visualize the rapid propagation of cracks in a PA11 strip specimen. The time t_0 is chosen as the reference point where the crack starts to propagate in dynamic regime. The time between two images is 10^{-4} s.

2.3 Fracture surface analysis

An optical microscope and a scanning electron microscope (SEM) are used to observe the fracture surfaces of the samples. Samples are taken from the cracked plates. They are embedded in acrylic resin and metallized in order to visualize them with the SEM. The apparatus used for metallization is a Cressington 108 auto. The gold layer is assumed to be of constant thickness on the surface of the sample. The optical microscope used is a Keyence VHX1000. The samples were then observed using a SEM (Zeiss EVOHD 15). An accelerated voltage of 10 keV is used with a current of 200 pA.

3 Results

A fracture surface was reconstructed using several observations by light microscopy (see Fig. 3). A long length of cracking in sample B3 was analysed. One can observe in Table 1 some information on the tests carried out on the specimens. Different zones can be distinguished. From left to right, one can observe a zone where the razor blade has penetrated, a so-called initiation zone (zone **1**) and a propagation zone. These different zones as well as a crack arrest zone were analyzed to qualitatively describe the majority of the mechanisms observed on a microscopic scale.

3.1 Crack initiation

The energy brought to the system allowing the crack initiation is composed of the elastic energy stored in the plate and the kinetic energy generated by the impact of the mass on the razor blade. The objective of the dynamic fracture test is to establish as quickly as possible a

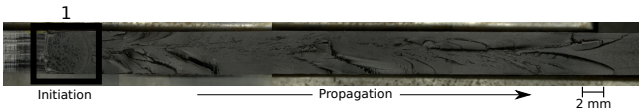

Figure 3. Observation by light microscopy of the fracture surface of sample B3. Zone 1 represents the crack initiation zone. The arrow indicates the direction of propagation.

stable state of propagation characterised by a constant energy release rate during propagation. From the point of view of crack length, this transition zone between initiation and propagation is negligible. This is the interest of a rapid propagation (i.e. dynamic fracture) test, to be able to free oneself from the crack initiation. Nevertheless, on a microscopic scale, the fracture surface reflects this abrupt transition. Several characteristic areas can be observed in Fig. 4. From left to right, we find the zone of penetration of the blade, the zone where conical marks can be observed, an intermediate zone called "mist zone" and a chaotic zone from the point of view of roughness called "hackle zone" [25] [26]. The area of conical markings and the hackle zone are considered to be associated with crack initiation and propagation, respectively. In the mist zone (see Fig. 5), plastic deformation of the resin is noticeable. This suggests that the material was stressed "slowly" and at a high level of deformation.

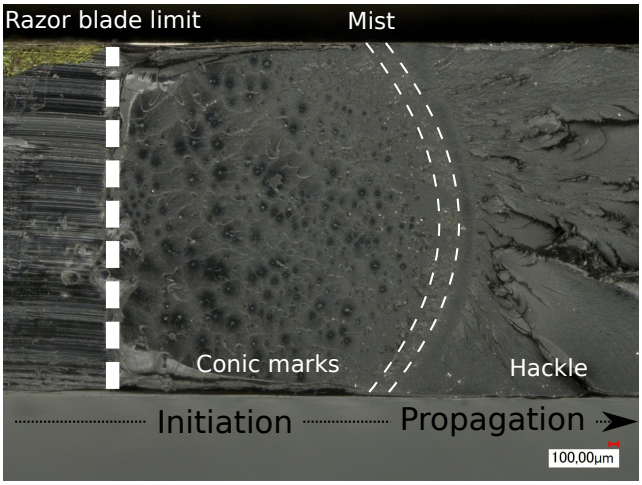

Figure 4. Several zones can be identified (from left to right): the razor blade penetration zone - the conical mark zone - the intermediate "mist" zone - the chaotic "hackle" zone. The arrow indicates the direction of propagation.

The additional energy generated by the impact of a mass on a razor blade allows the transition of the crack into a rapid propagation regime where the fracture surface is more chaotic. At this instant, the energy release rate is higher than the critical energy release rate associated with crack propagation in dynamic regime ($G_I > G_{IDc}$).

3.2 Crack propagation

The analysis of crack propagation is relatively simple from the point of view of external loading and space-time data of the crack tip. The energy release rate is assumed to be constant

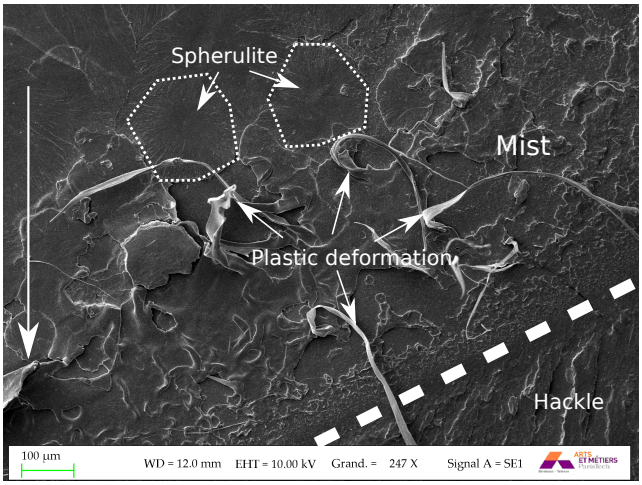

Figure 5. Observation by electron microscopy of the mist zone of the fracture surface of sample B4. Several zones can be identified (from top to bottom): the smooth zone with the appearance of spherulites (end of the zone of conical marks) - the mist zone with plastic deformation of the resin - a stop mark of the macro-crack in dotted line - the hackle zone. The long arrow on the left indicates the direction of propagation.

over almost the entire length of the crack. The crack is in a quasi-permanent regime of rapid propagation. Analysis of the fracture surface is more complex. This makes the estimation of the fracture energy hazardous.

The zone of propagation of the fracture surface of sample B5 is shown in Fig. 6. The main direction of the macrocrack front is indicated by the large white arrow at the top of the figure. The three small white arrows indicate the propagation directions of several microcracks. Characteristic river patterns in polymer resin composites can be seen in [27].

The description of crack propagation through a macro-front no longer seems at all relevant at this scale. Micro-cracks seem to propagate in different directions and planes. The interaction of several micro-cracks in planes at different altitudes seems to be at the origin of the river markings. Micro branches generating arrest marks are visible. This can be interpreted as a local stick slip phenomenon (see Fig. 7).

3.3 Estimation of the fracture energy

The fracture energy was estimated for 6 specimens (see Tab.1). For a macroscopic velocity of the order of $0.6c_R$, the fracture energy is not unique and varies from 9.4 to 15.6 kJm^{-2}. This can be explained by not taking into account the amount of surface area created by the crack in the fracture energy estimate. Only the amount of projected surface area (crack length multiplied by the thickness of the specimen) is considered.

3.4 Crack arrest

Fig. 8 shows a crack arrest. The large white arrow at the top indicates the main direction of propagation of the macrocrack front. The five small black arrows indicate the propagation directions of several micro-cracks. The dashed line indicates the area of crack arrest. To the right of the specimen, there is an area where the material has been plastically deformed due

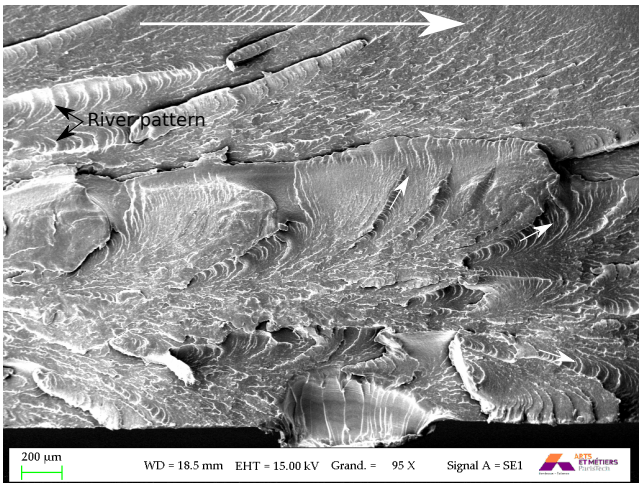

Figure 6. Observation by electron microscopy of the propagation zone of the fracture surface of sample B5. The large white arrow at the top indicates the main direction of propagation of the macrocrack front. The three small white arrows indicate the propagation directions of several microcracks. Characteristic river patterns in multi-phase polymers with high heterogeneity can be observed.

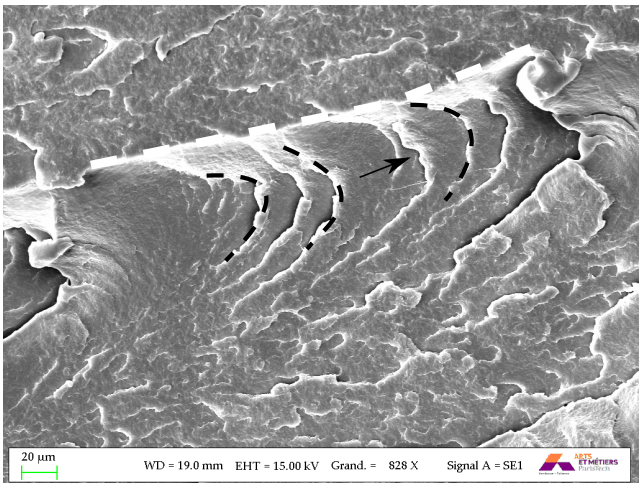

Figure 7. Observation by electron microscopy of the microcracks in the propagation zone of the fracture surface of sample B5. The arrow indicates the direction of propagation of the microcrack front. Several parabolic arrest marks of the micro-crack can be observed. The dashed line indicates the boundary between two crack planes at two different altitudes.

to the self-heating induced by the cutting of the specimen. The microcracks described in the previous section continue to propagate in different directions. However, they are less and less numerous as they approach the arrest zone. The surface is smoother than during propagation. Nevertheless, cracking planes are still present at different altitudes. Crack arrest is abrupt. The macrocrack front is no longer parabolic. Conventional rib marking known for PMMA cannot be identified.

Sample	δ	T	$\dot{a}$	$\dot{a}/c_R$	G_{I0}	G_{ID}
B3	2	19	390	0.55	10.4	9.4
B4	2	19	420	0.60	10.1	9.1
B5	2.3	20	400	0.57	12.2	11.0
B6	2.5	21	410	0.59	15.5	14.0
B7	2.5	20	380	0.54	16.2	14.6
B8	2.7	23	390	0.55	17.3	15.6

Table 1. Estimation of the fracture energy G_{ID} (kJm^{-2}), the quasi-static energy release rate G_{I0} (kJm^{-2}) as a function of the crack velocity $\dot{a}$ ((ms^{-1})), the temperature T (°C) and the displacement δ (mm) imposed during pre-loading.

Figure 8. Observation by electron microscopy of the arrest zone of a crack on the fracture surface of sample B7. The large white arrow at the top indicates the main direction of propagation of the macrocrack front. The five small black arrows indicate the directions of propagation of several micro-cracks. The dashed line indicates the arrest zone of the crack. To the right of the specimen is an area where the material has been plastically deformed as a result of cutting the specimen.

4 Discussion

The initiation areas of the fracture surfaces were analyzed. They confirm three distinct zones: a zone with conical markings, an intermediate zone (mist) and a chaotic zone (hackle). During the static pre-stressing of the sample, micro-cracks seem to develop from the nuclei of the spherulites. This (crystalline) phase of the material is assumed to be brittle. In contrast to the amorphous phase which brings ductility to the material when it is stressed relatively "slowly". These micro-cracks coalesce and interfere with a macro-front to generate conical marks which have been observed. The appearance of these micro-cracks, often associated with cavities, is described in the literature [28, 29]. The amorphous intra-spherolitic phase cavitates (or micro-crack) [30]. When the density of micro-cracks is critical, a macro-crack is created [31] [32]. This crack of a few mm ends up stopping in the mist zone, where plastic deformation of the matrix is found. The ductility of the amorphous phase eventually takes over the brittle (crystalline) phase of the material. This can be explained by the (quasi-static) strain rate and the degree of crystallinity (about 20 %). At this moment the energy release rate

is lower than the critical energy release rate allowing crack initiation ($G_I < G_{Ic}$). The polymer is therefore ductile under quasi-static regime. The external impact on the razor blade will provide the energy (and instability) necessary to initiate the crack in a dynamic propagation regime. This is evidenced by the observation of a chaotic zone in the surface roughness. The local strain rate induced by the rapid crack propagation probably causes a significant drop in the ductility of the amorphous phase. The amorphous and crystalline phases are then brittle. The energy release rate is this time higher than the critical energy release rate allowing the rapid propagation of the crack ($G_I > G_{IDc}$).

The difference in behaviour between crack initiation and rapid crack propagation for this type of material is considerable. Initiating a crack requires an energy release rate that is often very high compared to that which the material would require to sustain rapid crack propagation. This is due to a significant difference between the resistance to slow propagation (initiation) and rapid propagation of the material: $G_{Ic} > G_{IDc}$. These significant differences have been reported for other industrial materials [10]. In the area of rapid propagation, the propagation velocity of the macrocrack front is relatively constant ($\dot{a} \approx 0.6 c_R$). This critical velocity is a priori the limit at which the crack branches due to inertia effects [2]. The specimens studied show a longitudinal crack. Analysis of the fracture surface reveals a complex roughness. Numerous micro-cracks, micro-branches and arrest marks are observed. They appear in different crack planes. A single macro-crack front seems to be no longer identifiable. The material seeks to dissipate a significant amount of energy ($G_I >> G_{IDc}$) by cracking mostly in the amorphous phase. Spherulites, i.e. the crystalline phase, are heterogeneities that disturb the local stress field of the micro-crack tips. This induces micro-branches and micro-cracking phenomena in different planes in large numbers. This allows the material (i.e. the individual cracks) to dissipate *in fine* a large amount of energy. One could postulate that the material dissipates as much or more energy with a single crack with many micro-cracks and micro-branches than with macro-branches. This is probably why a longitudinal macro-crack could be generated in several samples despite $G_I >> G_{IDc}$. When the energy release rate is limited (in the crack arrest zones), the surfaces observed on a macroscopic scale become smooth.

5 Conclusions

The work described in this article focuses on the qualitative analysis of fracture surface. The cracks were generated by a dynamic fracture test. Strip band specimens known to generate very few inertia effects were used. The material studied is a semi-crystalline industrial biobased polymer: PA11. Its complex fracture behaviour ultimately resembles that of a large number of polymers used in industry. There is a significant difference in fracture behaviour between initiation and rapid propagation. This was evidenced by the analysis of the fracture surfaces. The mechanisms observed in the initiation and propagation zones are relatively well known. The influence of the highly heterogeneous microstructure of a semi-crystalline and the cracking regime induces a signature different from those described for the well-known homalite 100 and PMMA. The random organization of spherulites in the material confers relatively singular small-scale fracture mechanisms.

6 Acknowledgements

The authors would like to warmly thank the participation in this work of V. Honno and A. Bradu who did a Bachelor internship on the subject and J. Bega for his technical support on microscopic analyses.

7 Conflicts of interest

The authors declare that there are no conflicts of interest regarding the publication of this paper.

References

[1] P. Beguelin, C. Fond, H.H. Kausch, Journal de Physique IV **7**, 867 (1997)
[2] E.H. Yoffe, Philosophical Magazine **42**, 739 (1951)
[3] K.B. Broberg, Arkiv for Fysik **18**, 159 (1960)
[4] L.B. Freund, Journal of the Mechanics and Physics of Solids **20**, 129 (1972)
[5] J. Fineberg, E. Bouchbinder, International Journal of Fracture **196**, 33 (2015)
[6] M. Lebihain, J.B. Leblond, L. Ponson, Journal of the Mechanics and Physics of Solids **137** (2020)
[7] K. Ravi-Chandar, International Journal of Fracture **90**, 83 (1998)
[8] E. Sharon, J. Fineberg, Nature **397**, 333 (1999)
[9] J. Rice, Journal of Applied Mechanics, Transactions ASME **35**, 379 (1964)
[10] C. Fond, R. Schirrer, Notes au C.R.A.S., Series IIb **329**, 195 (2001)
[11] J.B. Kopp, C. Fond, G. Hochstetter, Engineering Fracture Mechanics **202**, 445 (2018)
[12] J. Kies, A. Sullivan, G. Irwin, Journal of Applied Physics **21**, 716 (1950)
[13] B. Yang, K. Ravi-Chandar, Journal of the Mechanics and Physics of Solids **44**, 1955 (1996)
[14] D. Dalmas, C. Guerra, J. Scheibert, D. Bonamy, International Journal of Fracture **184**, 93 (2013)
[15] C.M. Guerra Amaro, Theses, Ecole Polytechnique X (2009), `https://pastel.archives-ouvertes.fr/pastel-00006135`
[16] E. Sharon, J. Fineberg, Physical Review B - Condensed Matter and Materials Physics **54**, 7128 (1996)
[17] K. Ravi-Chandar, W. Knauss, International Journal of Fracture **26**, 65 (1984)
[18] J. Fineberg, M. Marder, Physics Reports **313**, 1 (1999)
[19] J.B. Kopp, J. Schmittbuhl, O. Noel, J. Lin, C. Fond, Engineering Fracture Mechanics **126**, 178 (2014)
[20] J.B. Kopp, J. Schmittbuhl, O. Noel, C. Fond, International Journal of Fracture **193**, 141 (2015)
[21] W. Bradley, W. Cantwell, H. Kausch, Mechanics Time-Dependent Materials **1**, 241 (1997)
[22] F. Nilsson, International Journal of Fracture **8**, 403 (1972)
[23] J.B. Kopp, J. Girardot, International Journal of Fracture **226**, 121 (2020)
[24] B. Cotterell, International Journal of Fracture Mechanics **4**, 209 (1968)
[25] J. Johnson, D. Holloway, Philosophical Magazine **14**, 731 (1966)
[26] K. Ravi-Chandar, W. Knauss, International Journal of Fracture **20**, 209 (1982)
[27] L. Barbosa, D. Bortoluzzi, J. Ancelotti, A.C., Composites Part B: Engineering **175** (2019)
[28] N. Selles, P. Cloetens, H. Proudhon, T.F. Morgeneyer, O. Klinkova, N. Saintier, L. Laiarinandrasana, Macromolecules **50**, 4372 (2017)
[29] P.A. Poulet, G. Hochstetter, A. King, H. Proudhon, S. Joannès, L. Laiarinandrasana, Polymer Testing **56**, 245 (2016)

[30] S. Castagnet, J.L. Gacougnolle, P. Dang, Materials Science and Engineering: A **276**, 152 (2000)
[31] S.N. Zhurkov, V.S. Kuksenko, International Journal of Fracture **11**, 629 (1875)
[32] S.N. Zhurkov, V.A. Zakrevskyi, V.E. Korsukov, V.S. Kuksenko, Journal of Polymer Science Part A-2: Polymer Physics **10**, 1509 (1972)